Biochemistry

 Volume 38, Number 50 December 14, 1999

Accelerated Publications

Potentiometric Analysis of the Flavin Cofactors of Neuronal Nitric Oxide Synthase†

Michael A. Noble,‡ Andrew W. Munro,§ Stuart L. Rivers,‡ Laura Robledo,‡ Simon N. Daff,‡ Lesley J. Yellowlees,‡ Toru Shimizu,|| Ikuko Sagami,|| J. Guy Guillemette,⊥ and Stephen K. Chapman*,‡

Department of Chemistry, University of Edinburgh, West Mains Road, Edinburgh EH9 3JJ, U.K., Department of Pure & Applied Chemistry, University of Strathclyde, The Royal College, 204 George Street, Glasgow G1 1XL, U.K., Institute of Chemical Reaction Science, Tohoku University, Sendai, Japan, and Department of Chemistry, University of Waterloo, Waterloo, Ontario N2L 3G1, Canada

Received September 15, 1999; Revised Manuscript Received October 25, 1999

ABSTRACT: Midpoint reduction potentials for the flavin cofactors in the reductase domain of rat neuronal nitric oxide synthase (nNOS) in calmodulin (CaM)-free and -bound forms have been determined by direct anaerobic titration. In the CaM-free form, the FMN potentials are −49 ± 5 mV (oxidized/semiquinone) −274 ± 5 mV (semiquinone/reduced). The corresponding FAD potentials are −232 ± 7, and −280 ± 6 mV. The data indicate that each flavin can exist as a blue (neutral) semiquinone. The accumulation of blue semiquinone on the FMN is considerably higher than seen on the FAD due to the much larger separation (225 mV) of its two potentials (cf. 48 mV for FAD). For the CaM-bound form of the protein, the midpoint potentials are essentially identical: there is a small alteration in the FMN oxidized/semiquinone potential (−30 ± 4 mV); the other three potentials are unaffected. The heme midpoint potentials for nNOS [−239 mV, L-Arg-free; −220 mV, L-Arg-bound; Presta, A., Weber-Main, A. M., Stankovich, M. T., and Stuehr, D. J. (1998) *J. Am. Chem. Soc. 120*, 9460−9465] are poised such that electron transfer from flavin domain is thermodynamically feasible. Clearly, CaM binding is necessary in eliciting conformational changes that enhance flavin to flavin and flavin to heme electron transfers rather than causing a change in the driving force.

Nitric oxide (NO) is a key signaling molecule in a diverse array of cellular processes. These range from essential roles in signal transduction in the nervous system to blood pressure regulation and involvement in the immune response (for a review, see ref *1*). It is synthesized in mammals by the nitric oxide synthases, a highly regulated family of enzymes of which three isoforms are known. These are nNOS (neuronal) and eNOS (endothelial), both of which are constitutively expressed and regulated posttranslationally, and iNOS (inducible), which is regulated at the level of transcription and produced in response to certain stimuli (e.g., cytokines) (*2*).

The NOS enzymes are flavocytochromes and contain both FAD and FMN as well as a P450[1]-like cysteine thiolate-ligated protoporphyrin IX (*3*−*7*). They have a bi-domain structure, composed of a heme domain tethered by a linker

† This work was supported by the U.K. Biotechnology and Biological Sciences Research Council (BBSRC) and by the National Sciences and Engineering Research Council of Canada.

* Author for correspondence. E-mail: S.K.Chapman@ed.ac.uk. Tel/Fax: 00 44 131 650 4760.

‡ University of Edinburgh.

§ University of Strathclyde.

|| Tohoku University.

⊥ University of Waterloo.

[1] Abbreviations: IPTG, isopropyl-β-D-thiogalactopyranoside; OD, optical density; PMSF, phenylmethanesulfonyl fluoride; P450, cytochrome P450 monooxygenase; SHE, standard hydrogen electrode.

10.1021/bi992150w CCC: $18.00
Published on Web 11/20/1999

region to a diflavin domain. The diflavin domain is highly homologous to NADPH-cytochrome P450 reductase (*8*). NOSs catalyze the oxidation of L-arginine to L-citrulline and NO. This requires NADPH and molecular oxygen in a complex mechanistic cycle that involves two successive oxidative steps: the first is a classical P450 hydroxylation and uses 1 equiv of NADPH and oxygen to form *N*-hydroxy-L-arginine; the unique second step uses 0.5 equiv NADPH and 1 equiv oxygen to oxidize *N*-hydroxy-L-arginine to yield L-citrulline and NO (*9*−*13*). Only the dimeric form of the enzyme is functionally active (*14*). The reason for this is that electron transfer occurs from the flavin domain of one monomer to the heme domain of the other (*15*). Tetrahydrobiopterin (H_4B) and calmodulin (CaM) are also catalytically essential cofactors. H_4B binds in the heme domain within the active site close to the substrate arginine, and although its precise role remains uncertain, it seems to be essential for catalytically competent dimer assembly (*16*, *17*). CaM binds tightly to an amphipathic α-helical region containing 12 basic and hydrophobic residues located in the linker region between the reductase and heme domains (*18*). For nNOS and eNOS, only Ca^{2+}-bound CaM can bind to and activate the enzyme, but for iNOS, the CaM remains tightly bound in the absence of Ca^{2+} (*19*). The activating function of CaM binding is complete within the reductase-linker domain itself: for CaM-bound nNOS reductase, there is increased cytochrome *c* and ferricyanide reductase activity (*20*), and there is an increased rate of flavin reduction by NADPH (*21*), as compared with the CaM-free form.

Recently, a comparative study of the effects of L-Arg and H_4B binding on the heme midpoint potentials showed an important difference between the heme domains of iNOS and nNOS (*22*). In the substrate- and H_4B-free forms, the reduction potential for iNOS (−347 mV) is some 100 mV lower than that for the nNOS (−239 mV). The binding of L-Arg results in a dramatic increase in the reduction potential for iNOS (up to −235 mV), almost exactly to the same value as that for the nNOS. The reduction potential for nNOS remains unaffected by L-Arg binding. These important results point to a key difference in the way these two enzymes regulate electron transfer to the heme and hence catalyze NO production. They indicate that the electron transfer from flavin to heme in iNOS is regulated by a substrate-induced thermodynamic switch, the same mechanism as that operative in P450cam (*23*, *24*) and P450 BM3 (*25*). No such mechanism exists for control of electron transfer to the heme in nNOS, and an alternative regulatory mechanism involving the binding of Ca^{2+}-activated calmodulin has been shown to trigger the flavin to heme electron transfer (*26*).

In this paper, we present a study of the thermodynamic properties of the flavin cofactors in neuronal NOS in the CaM-free and CaM-bound forms, resolving the regulatory role of CaM. We demonstrate that each of the two flavins can exist with a stable blue (neutral) semiquinone. The titration data permit the resolution and assignment of all four midpoint potentials (2 × oxidized/semiquinone and 2 × semiquinone/reduced). CaM binding has little effect on the potentials and this establishes its role as a purely conformational effector.

EXPERIMENTAL PROCEDURES

Overexpression of nNOS in Escherichia coli. Plasmid pCRNNR (*27*) expressing rat nNOS reductase domain (residues 695−1429 that encompass the calmodulin binding linker region) was used to transform strain JM109. Typically protein was purified from a total of 2 L of transformant cell culture (5 × 400 mL of LB medium containing ampicillin (50 μg/mL). Cells were grown to an OD_{600} of 0.8 at 37 °C and induced with IPTG (100 μg/mL) and incubated with rapid shaking at 30 °C for 24 h. Cells were harvested by centrifugation, washed with 50 mM Tris-HCl (7.4), and stored at −20 °C.

Protein Preparation. Frozen *E. coli* cells were thawed, resuspended in 80−100 mL of chilled lysis buffer [50 mM Tris-HCl (7.4) containing 10% glycerol, 1 mM EDTA, and 1 mM PMSF] and disrupted on ice using a Sanyo Soniprep 150 sonicator. A three-column regime was used for protein purification. Cell debris was pelletted by centrifugation (18 000 rpm, at 4 °C for 30 min), the soluble cell extract was loaded directly onto a DEAE-Sephacel column (Sigma) (2.5 × 15 cm), and unbound protein was removed by flushing the column with 200 mL of lysis buffer. Bound protein was eluted using a salt gradient of 0−500 mM KCl, and 5-mL fractions were collected. Fractions containing yellow-green protein were assayed for cytochrome *c* activity at 550 nm in the presence (plus 5 mM $CaCl_2$) and the absence (plus 1 mM EDTA) of calmodulin to confirm the calmodulin-stimulated nNOS reductase activity. Active fractions were loaded directly onto an ADP−Sepharose column (1.5 × 4 cm), and unbound material was removed by flushing with at least 100 mL of the 50 mM Tris-HCl (7.4) buffer. Bound protein was removed in a small (ca. 5 mL) volume by washing with the 50 mM Tris-HCl containing 10 mM $NADP^+$. To remove all the tightly bound $NADP^+$, the protein was dialyzed against 2 L of 10 mM potassium phosphate (6.8) containing 1 mM EDTA and 10% v/v glycerol and loaded onto a hydroxyapatite column (2.5 × 10 cm) equilibrated with the same phosphate buffer. The column was washed with 500 mL of buffer and the bound protein eluted using a gradient from 10 to 500 mM potassium phospate (6.8), again containing 1 mM EDTA and 10% v/v glycerol. Yellow−green fractions were pooled, and the protein sample was concentrated to ca. 3 mL and stored frozen at −80 °C.

Spectroscopic Studies. Absorbance spectra and activity assays of chromatographic fractions of partially pure protein and samples of purified nNOS reductase were measured on a Shimadzu 2101 UV−visible spectrophotometer. Cytochrome *c* (horse heart, type I; Sigma) reductase activities were measured at 550 nm ($\Delta\epsilon_{550}$ = 22.64 mM^{-1} cm^{-1}) at 30 °C in 50 mM Tris-HCl (7.4) and also in the presence of various concentrations (up to 5% v/v) of Tween 20 (Sigma). Circular dichroism spectra of the nNOS reductase were measured on a Jasco J-600 spectrapolarimeter in the near (260−600 nm) and far UV (190−260 nm) regions, in 50 mM Tris-HCl (7.1) containing 10% v/v glycerol and various concentrations (up to 5% v/v) of Tween 20.

Potentiometric Titrations. Redox titrations were performed within a Belle Technology glovebox under a nitrogen atmosphere with oxygen maintained at less than 5 ppm. Titrations were performed in 50 mM Tris-HCl containing

100 mM KCl, 10% glycerol, and 0.5% Tween20 (Sigma) (pH 7.1) (titration buffer) at 25 ± 1 °C. Spectra (370−750 nm) were recorded on a Shimadzu 2101 UV−visible spectrophotometer, and the electrochemical potential was monitored using a CD740 m coupled to a Russell Pt/calomel combination electrode. The electrode was calibrated using the Fe(II)/Fe(III)−EDTA couple as a standard (108 mV), and the measured potentials were corrected to those for the standard hydrogen electrode (SHE) (Pt/calomel electrode + 244 mV). Protein solutions were titrated electrochemically using the method of Dutton (*28*) with sodium dithionite as the reductant and potassium ferricyanide as the oxidant.

For the titration of CaM-free nNOS reductase, the titration buffer also contained 1 mM EDTA. The protein sample was made ready for titration by exchange of the phosphate storage buffer to the titration buffer by elution through a Sephadex G25 column (1.5 × 20 cm) prior to introduction to the glovebox. For the titration of the nNOS reductase in the presence of calmodulin, the EDTA was replaced with 2 mM $CaCl_2$, and the protein sample was readied for the experiment by passing through two G25 columns: the first to exchange the phosphate for the titration buffer (in the presence of EDTA) and the second to exchange the 1 mM EDTA for 2 mM $CaCl_2$. Following this step, calmodulin (high-purity, bovine brain; Calbiochem) was added to a final concentration in slight excess over that of the reductase, and the protein was concentrated to ca. 2 mL prior to introduction to the glovebox. Following admission to the glovebox, concentrated protein samples were immediately passed through an anaerobic Sephadex G25 column, using degassed titration buffer, thereby removing all traces of oxygen. Typical sample volume for titration was 8−10 mL. The mediators benzyl viologen (BV), methyl viologen (MV), 2-hydroxy-1,4-naphthaquinone (HNQ), and phenazine methosulfate (PMS) (0.5 μM for each) were added prior to titration. For the reductive titration, the sample was initially fully oxidized by the addition of small aliquots of potassium ferricyanide until the potential had stabilized to ca. 200 mV (relative to SHE). After addition of each aliquot of sodium dithionite and allowing for equilibration/stabilization of observed potential, 2 mL of the protein solution was transferred to a cuvette, a spectrum was recorded, and the solution was returned to the titration beaker. Small corrections were made for any drift in the baseline by correcting the absorbance at 800 nm to zero.

Treatment of Absorbance−Potential Data. All data manipulations and nonlinear least-squares curve-fitting were performed using Origin (Microcal). From the set of spectra obtained from the reductive titrations, absorbance values at 458 nm (λ_{max} for oxidized flavin) and at 592 nm (λ_{max} for blue semiquinone) were plotted against potential. The 458 nm plots were fitted to the 4-electron equation (eq 1). The 592 nm plots were fitted to eq 2, which represents the sum of two 2-electron equations (eq 2). Both of these equations were derived by extension of the single-electron Nernst equation and the Beer−Lambert law for two and four sequential redox steps:

$$A = [a10^{(2E-E_1'-E_2')/59} + b10^{(E-E_2')/59} + c + d10^{(E_3'-E)/59} + e10^{(E_3'+E_4'-2E)/59}]/[1 + 10^{(2E-E_1'-E_2')/59} + 10^{(E-E_2')/59} + 10^{(E_3'-E)/59} + 10^{(E_3'+E_4'-2E)/59}] \quad (1)$$

$$A = \frac{a10^{(E-E_1')/59} + b + c10^{(E_2'-E)/59}}{1 + 10^{(E-E_1')/59} + 10^{(E_2'-E)/59}} + \frac{d10^{(E-E_3')/59} + e + f10^{(E_4'-E)/59}}{1 + 10^{(E-E_3')/59} + 10^{(E_4'-E)/59}} \quad (2)$$

where A is the total absorbance. In eq 1, $a-e$ are the relative absorbance values contributed by the diflavin in each of five nondegenerate oxidation states. In eq 2, $a-c$ are the relative absorbance values contributed by each of three oxidation states (ox, sq, hq) of one flavin; and $d-f$ are the equivalent values of the second flavin. In both equations, $E_1'-E_4'$ are the four midpoint potentials, two for each flavin.

RESULTS AND DISCUSSION

Optimizing Titration Conditions. Preliminary redox titration experiments were hampered by a tendency of the nNOS reductase to aggregate and precipitate over the period of several hours required to complete a titration. This was overcome by inclusion of a small amount of Tween 20 in the titration buffer (0.5% v/v). We observed that the addition of Tween 20 in the assay buffer at least up to levels of 5% has no measurable effect on the kinetic parameters for cytochrome *c* reduction catalyzed by both the nNOS reductase and a full-length nNOS expressed in yeast. In addition, there is no effect on the far-UV or near-UV−visible CD spectra of nNOS reductase in buffer containing 0.5% Tween 20, although at a level of 5% Tween 20 the far-UV CD spectrum indicates a small change in secondary structure. Therefore, we are confident that 0.5% Tween 20 has a negligible effect on the midpoint potentials.

Titrations and Data Analysis. Samples of purified, concentrated nNOS reductase appear dark green in color due to an air stable semiquinone. The apparent potential of such a solution (prior to full oxidation by the addition of potassium ferricyanide) is typically ca. 90 mV. Addition of the minimum amount of ferricyanide to fully oxidize the flavin (as judged by the color change to yellow) and allowing equilibration to occur yields a solution with a measured potential significantly more negative than 90 mV. Clearly, the semiquinone can exist because it is kinetically inert to oxidation by dioxygen.

A set of titration spectra was obtained after the addition of the minimum amount of ferricyanide to effect full oxidation. After the addition of each aliquot of dithionite, a spectrum was recorded and the potential noted; this process was repeated until it was clear that both flavins were fully reduced. Full-range oxidative titrations following reduction of the flavins were problematic; however, spectra obtained from reoxidation of partially reduced nNOS reductase over a limited potential range (ca. −100 to + 50 mV) clearly matched those of the reductive titration.

A selection of spectra for a typical reductive titration of calmodulin-free nNOS reductase is shown in Figure 1. The broad band with a maximum at 458 nm, typical of a flavoprotein, is most intense in the fully oxidized form of the protein. The high wavelength band, maximal at 592 nm, is indicative of the blue (neutral) semiquinone species. Plots of the absorbance at each of these two wavelengths versus potential are shown in Figure 2. The dependence on potential of the absorbance at 458 nm is double-sigmoidal in form

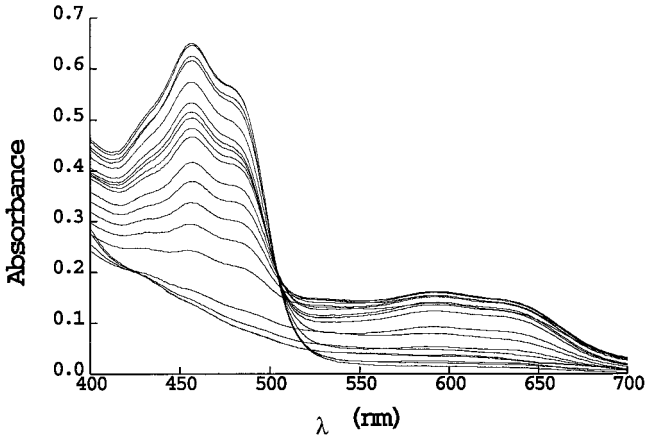

FIGURE 1: Absorption spectra for the redox titration of calmodulin-free nNOS in 50 mM Tris-HCl containing 10% v/v glycerol and 0.5% v/v Tween 20 (pH 7.1), obtained as described in Experimental Procedures.

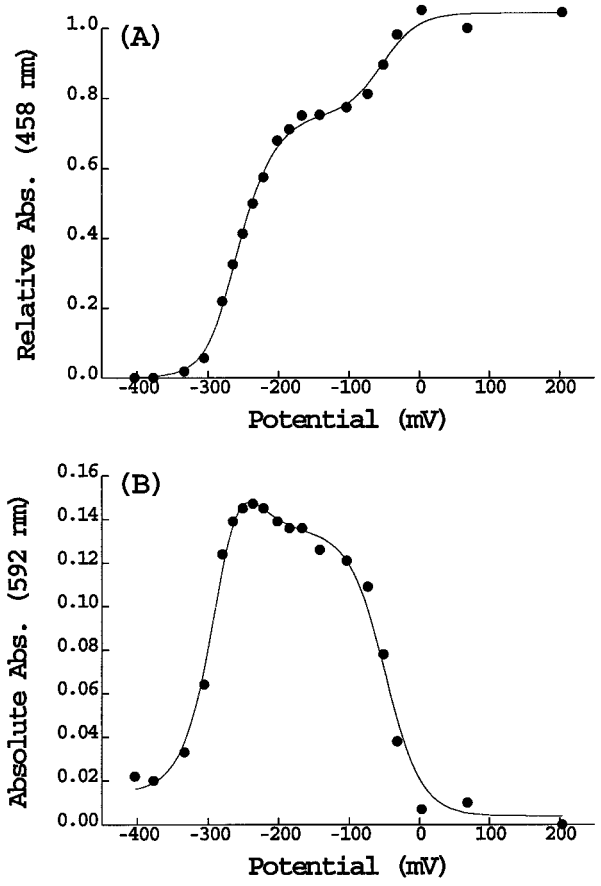

FIGURE 2: Plots of (A) relative absorbance at 458 nm and (B) absolute absorbance at 592 nm against potential for the redox titration of calmodulin-free nNOS reductase. Data are fitted using eqs 1 and 2 (solid line) as described in the text, and the midpoint potentials are shown in Table 1.

(Figure 2A). The sigmoidal wave spanning the lower potential range contributes approximately three-quarters of the overall absorbance change and that spanning the higher potential wave was the remaining one-quarter. The four component midpoint potentials and five associated component absorbance values are calculated by fitting the data to the 4-electron equation (eq 1) (assuming 4 sequential 1-electron steps). It is valid to make the assumption that the magnitudes of the absorbance for the oxidized/semiquinone

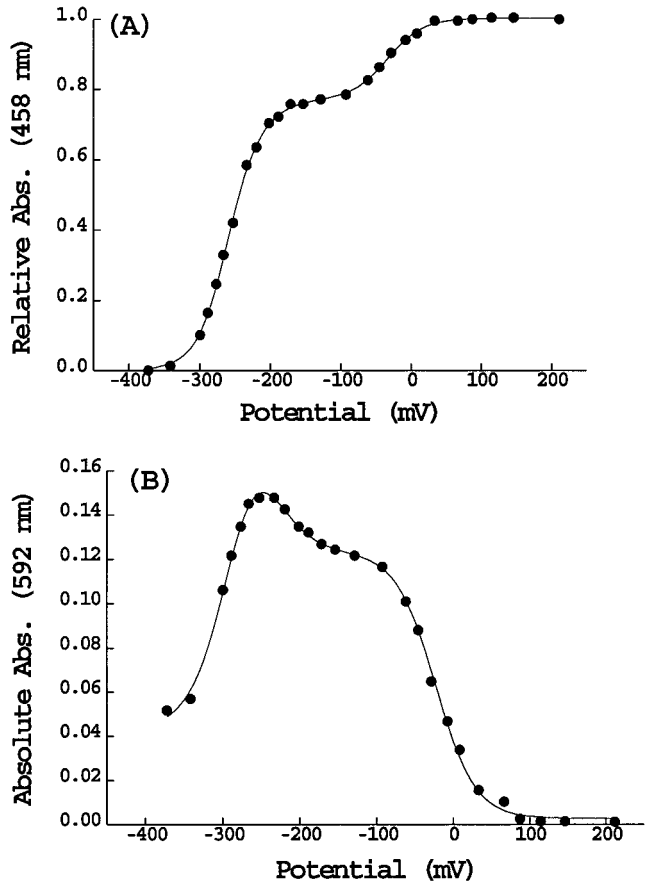

FIGURE 3: Plots of (A) relative absorbance at 458 nm and (B) absolute absorbance at 592 nm against potential for the redox titration of calmodulin-bound nNOS reductase. Data are fitted using eqs 1 and 2 (solid line) as described in the text, and the midpoint potentials are shown in Table 1.

and for the semiquinone/reduced couples for each of the flavins are approximately equal and to constrain the absorbance limits in the fitting process accordingly. These restrictions forbid unrealistic fitting, particularly in the lower potential range where there are three closely similar midpoint potentials. The plot of the absorbance at 592 nm versus potential (Figure 2B) consists of a broad bell-shaped curve that clearly contains two separate and overlapping semiquinone contributors. A composite equation of two separate 2-electron terms (eq 2) was used to fit these data.

Plots of the relative absorbance at 458 nm and absolute absorbance at 592 nm versus potential for the CaM-bound nNOS reductase are shown in Figure 3. The same fitting procedures as outlined above were used to determine the midpoint potentials for these data.

The midpoint potentials derived from both plots for each reductive titration are collated in Table 1. The values determined from the A_{458}−potential plots fitted using eq 1 and from the A_{592}−potential plots fitted using eq 2 were in close agreement. The values quoted are the mean of those generated by utilizing a range of different absorbance constraints in fitting using eqs 1 and 2.

It is clear that the A_{592}−potential plots (Figures 2B and 3B) contain two components, demonstrating that each flavin can exist as a blue semiquinone. As a consequence, and by analogy with cytochrome P450 reductase, it is possible to assign the determined midpoint potentials to specific flavins.

Table 1: Midpoint Reduction Potentials vs SHE (25 °C, pH 7.1) for the Flavins of Rat nNOS Reductase Domain in the Calmodulin-Free and -Bound Forms[a]

	flavin midpoint potentials (mV)			
	FMN		FAD	
	ox/sq	sq/hq	ox/sq	sq/hq
−CaM	−49 ± 5	−274 ± 5	−232 ± 7	−280 ± 6
+CaM	−30 ± 4	−267 ± 5	−234 ± 6	−284 ± 9

[a] Determined from the absorbance−potential data shown in Figures 2 and 3 as described in the text.

Table 2: Flavin Midpoint Potentials of nNOS Reductase and Related Systems

	flavin midpoint potential (mV)				
	FMN		FAD		
diflavin reductase	ox/sq	sq/hq	ox/sq	sq/hq	ref
nNOS (−CaM)	−49	−274	−232	−280	present
P450 BM3	−193	−213	−292	−372	*25*
rabbit P450	−109	−279	−274	−371	*34*
sulfite reductase	−152	−327	−382	−322	*35*

In the catalytic cycle of P450 and NOS, electrons are transferred to FAD from NADPH (as hydride), then to FMN and then to heme. For nNOS, this pathway has been clearly demonstrated by study of FMN-deficient mutants of nNOS (*29*). The FMN must be the high potential flavin since its role is to transfer electrons from the FAD to the heme. We can assign the highest midpoint potential (−49 mV, CaM-free; −30 mV, CaM-bound) to the FMN oxidized/semiquinone couple. Of the cluster of three lower potentials, those with values −232 and −280 mV (CaM-free) must be ascribed to the oxidized/semiquinone and semiquinone/reduced couples of the FAD, since they are the two with sufficient separation to allow the observation of a blue semiquinone. The remaining potential (−274 mV; CaM-free) is that characterizing the FMN semiquinone/reduced couple. Hence, the FMN contributes the major component and the FAD contributes the minor component of the semiquinone signal depicted in the A_{592}−potential plots (Figures 2B and 3B). The midpoint potential for the reduction of the FAD semiquinone lies at −280 mV, implying that facile reduction by NADPH (reduction potential −320 mV) can occur. However, Gachhui et al. (*20*) noted that the nNOS reductase domain was not fully reduced in the presence of excess NADPH but required the addition of dithionite to complete the reduction of the FAD semiquinone. Nevertheless, it is clear in Figure 1 that, toward the end of the redox titration, the reductase domain does approach full reduction. It is possible that $NADP^+$ or NADPH binding stabilizes the FAD semiquinone by shifting the reduction potential to a more negative value. Similar effects have been reported previously in P450 BM3 (*30*), adrenodoxin reductase (*31*), and cytochrome b_5 reductase (*32*).

Implications for nNOS Mechanism. These results clearly demonstrate that CaM binding has no effect on the flavin midpoint potentials (except that E_1', the FMN oxidized/semiquinone couple, appears to be shifted slightly to a more positive potential, from −54 to −34 mV). It can be concluded, therefore, that the regulatory role played by calmodulin in controlling the flavin (FMN) to heme electron transfer in nNOS is imposed as a structural rearrangement rather than a thermodynamic switch. Although we cannot rule out the possibility that the flavin redox characteristics in the holoenzyme are different to those of the isolated reductase, studies have shown that CaM binding induces similar changes in both forms, i.e., in fluorescence spectra and reductase activity (*20*, *29*). The flavin fluorescence increase originates from the FMN subdomain, since there is no such increase for FMN-deficient mutant forms of the reductase. CaM binding also results in both increases in flavin reduction rate by NADPH and steady-state reduction of artificial electron acceptors such as cytochrome *c* and ferricyanide (*20*, *29*). Our results show that; in the absence of bound CaM, the high FMN potential (−274 mV) is poised such that the first electron transfer to the ferric heme iron is thermodynamically feasible [$E'_{m,7}$ is −239mV for Fe(II)/Fe(III) couple in nNOS (*22*)] but which is prevented kinetically. Presumably, a favorable electron pathway is presented in response to CaM-promoted structural rearrangement. Furthermore, the redox state of the FMN immediately prior to commencement of the catalytic cycle on the heme must be the fully reduced (hydroquinone) to provide a thermodynamically accessible electron to the heme. Due to the proximity of the FAD potentials, the FMN will fluctuate between semiquinone and reduced states, with only the fully reduced state capable of delivering the first electron to the heme. The high FMN midpoint potential (−30 mV, CaM-bound) can only be accessed by the ferric superoxy species in the catalytic pathway, and so the oxidized/semiquinone form of the FMN provides the second flavin to heme electron transfer to generate the oxyferryl intermediate. The redox cycle of the reductase domain would therefore be completed by electron transfer from the FAD semiquinone to the oxidized FMN. The redox potential of the FAD oxidized/semiquinone couple is poised so that electron transfer to form the FMN semiquinone/hydroquinone is unfavorable, suggesting that two-electron cycling of both flavins occurs during catalysis. There is compelling evidence that the pathway is from the flavin domain of one monomer to the heme of the other and this is the reason only the dimeric enzyme assembly is active in synthesizing nitric oxide (*15*). For iNOS, the CaM has such a high affinity that it remains bound even in the absence of Ca^{2+}, but flavin to heme electron transfer does not occur until L-Arg binds and the reduction potential of the heme is elevated above the flavin. For CaM-bound, L-Arg-free dimeric nNOS, uncoupled flavin to heme electron transfer occurs generating superoxide (*33*).

Comparison with Redox Properties of Other Flavoenzymes. We can compare the redox properties of the diflavin domain of nNOS with those previously determined for the structurally related cytochrome P450 reductases, from rabbit (*34*) and from P450 BM3 (*25*), and with NADPH−sulfite reductase flavoprotein (*35*) (Table 2). Like those of rat nNOS reductase, each flavin in rabbit cytochrome P450 reductase titrates with a blue semiquinone. The highest of the four potentials, corresponding to the one-electron reduced form, is some 50 mV more negative than the analogous potential of nNOS reductase, and the lowest, −371 mV, is about 90 mV more negative than the lowest potential of nNOS reductase. In P450 BM3, only the FAD can exist as a blue semiquinone (midpoint potentials of −292 and −372 mV are well enough separated) whereas the FMN potentials are

closer together (−193 and −213 mV) and it essentially titrates from fully oxidized to fully reduced in a two-electron transition. On the other hand, for sulfite reductase flavoprotein, the redox potentials are such that the FMN cofactor can exist as a blue semiquinone whereas the FAD titrates from oxidized to reduced in a two-electron transition. All these data together indictate that clear differences in flavin redox characteristics exist among these reductase systems, despite their high structural homology. It remains to be seen whether the redox characteristics of the flavins in the different NOS isoforms iNOS and eNOS are similar to those of the flavins in nNOS.

We have reported the first determination of the flavin midpoint potentials for the reductase domain of a NOS isoform. Each flavin can exist with a stable neutral blue semiquinone, and the potentials are sufficiently well separated that they can be distinguished by titration of the intact FAD- and FMN-containing reductase. The midpoint potentials are not significantly perturbed by the presence of bound calmodulin, indicating that its role is as a structural effector of electron transfer in nNOS, altering orientation of the flavins to facilitate electron transfer.

REFERENCES

1. Ignarro, L., and Murad F., Eds. (1995) *Advances in Pharmacology, Volume 34. Nitric oxide: Biochemistry, molecular biology and therapeutic implications*, Academic Press, San Diego, CA.
2. Griffith, O. W., and Stuehr, D. J. (1995) *Annu. Rev. Physiol. 57*, 707−736.
3. Mayer, B., Mathias, J., Heinzel, B., Werner, E. R., Wachter, H., Schultz, G., and Böhme, E. (1991) *FEBS Lett. 288*, 187−191.
4. McMillan, K., Bredt, D. S., Hirsch, D. J., Synder, S. H., Clark, J. E., and Masters, B. S. S. (1992) *Proc. Natl. Acad. Sci. U.S.A. 89*, 11141−11145.
5. White, K. A., and Marletta, M. A., (1992) *Biochemistry 31*, 6627−6631.
6. Stuehr, D. J., and Ikeda-Saito, M. (1992) *J. Biol. Chem. 267*, 20547−20550.
7. Klatt, P., Schmidt, K., and Mayer, B. (1992) *Biochem. J. 288*, 15−17.
8. Bredt, D. S., Hwang, P. M., Glatt, C. E., Lowenstein, C., Reed, R. R., and Snyder, S. H. (1991) *Nature 351*, 714−718.
9. Kwon, N. S., Nathan, C. F., Gilker, C., Griffith, O. W., Matthews, D. E., and Stuehr, D. J. (1990) *J. Biol. Chem. 265*, 13442−13445.
10. Stuehr, D. J., Kwon, N. S., Nathan, C. F., Griffith, O. W., Feldman, P. L., and Wiseman, J. (1991) *J. Biol. Chem. 266*, 6259−6263.
11. Klatt, P., Schmidt, K., Uray, G., and Mayer, B. (1993) *J. Biol. Chem. 268*, 14781−14787.
12. Marletta, M. A. (1993) *J. Biol. Chem. 268*, 12231−12234.
13. Korth, H. G., Sustmann, R., Thater, C., Butler, A. R., and Ingold, K. U. (1994) *J. Biol. Chem. 269*, 17776−17779.
14. Klatt, P., Pfeiffer, S., List, B. M., Lehner, D., Glatter, O., Bachinger, H. P., Werner, E. R., Schmidt, K., and Mayer, B. (1996) *J. Biol. Chem. 271*, 7336−7342.
15. Siddhanta, U., Presta, A., Fan, B. C., Wolan, D., Rousseau, D. L., and Stuehr, D. J. (1998) *J. Biol. Chem. 273*, 18950−18958.
16. McMillan, K., and Masters, B. S. S. (1995) *Biochemistry 34*, 3686−3693.
17. Mayer, B., Wu, C. Q., Gorren, A. C. F., Pfeiffer, S., Schmidt, K., Clark, P., Stuehr, D. J., and Werner, E. R. (1997) *Biochemistry 36*, 8422−8427.
18. Vorherr, T., James, P., Krebs, J., Enyedi, A., McCormick, D. J., Penniston, J. T., and Carafoli, E. (1990) *Biochemistry 29*, 55−365.
19. Cho, H. J., Xie, Q. W., Calaycay, J., Mumford, R. A., Swiderek, K. M., Lee, T. D., and Nathan, C. (1992) *J. Exp. Med. 176*, 599−604.
20. Gachhui, R., Presta, A., Bentley, D. F., Abu-Soud, H. M., McArthur, R., Brudvig, G., Ghosh, D. K., and Stuehr, D. J. (1996) *J. Biol. Chem. 271*, 20594−20602.
21. Abu-Soud, H. M., Yoho, L. L., and Stuehr, D. J. (1994) *J. Biol. Chem. 269*, 32047−32050.
22. Presta, A., Weber-Main, A. M., Stankovich, M. T., and Stuehr, D. J. (1998) *J. Am. Chem. Soc. 120*, 9460−9465.
23. Sligar, S. G., and Gunsalus, I. C. (1976) *Proc. Natl. Acad. Sci. U.S.A. 73*, 1078−1082.
24. Martinis, S. A., Blanke, S. R., Hager, L. P., and Sligar, S. G. (1996) *Biochemistry 35*, 14530−14536.
25. Daff, S. N., Chapman, S. K., Turner, K. L., Holt, R. A., Govindaraj, S., Poulos, T. L., and Munro, A. W. (1997) *Biochemistry 36*, 13816−13823.
26. Abu-Soud, H. M., and Stuehr, D. J. (1993) *Proc. Natl. Acad. Sci. U.S.A. 90*, 10769−10772.
27. Newton, D. C., Montgomery, H. J., and Guillemette, J. G. (1998) *Arch. Biochem. Biophys. 359*, 249−257.
28. Dutton, P. L. (1978) *Methods Enzymol. 54*, 411−435.
29. Adak, S., Ghosh, S., Abu-Soud, H. M., and Stuehr, D. J. (1999) *J. Biol. Chem. 274*, 22313−22320.
30. Murataliev, M. B., Klein, M., Fulco, A. J., and Feyereisen, R. (1997) *Biochemistry 36*, 8401−8412.
31. Lambeth, J. D., and Kamin, H. (1976) *J. Biol. Chem. 251*, 4299−4306.
32. Iyanagi, T. (1977) *Biochemistry 16*, 2725−2730.
33. Gorren, A. C. F., List, B. M., Schrammel, A., Pitters, E., Hemmens, B., Werner, E. R., Schmidt, K., and Mayer, B. (1996) *Biochemistry 35*, 16735−16745.
34. Iyanagi, T., Makino, N., and Mason, H. S. (1974) *Biochemistry 13*, 1701−1710.
35. Zeghouf, M., Fontecave, M., Macherel, D., and Coves, J. (1998) *Biochemistry 37*, 6114−6123.

BI992150W